

7. de Vaucouleurs, G. *Astrophys. J.* **227**, 729–755 (1979).
 8. Sandage, A. & Tammann, G. A. *Astrophys. J.* **194**, 559–568 (1974).
 9. Ondrechen, M. P. *Astr. J.* **90**, 1474–1480 (1985).
 10. Sukumar, S., Klein, U. & Gräve, R. *Astr. Astrophys.* **184**, 71–78 (1987).
 11. Rybicki, G. B. & Lightman, A. P. *Radiative Processes in Astrophysics* 167–185 (Wiley-Interscience, New York, 1979).
 12. Segalovitz, A., Shane, W. W. & de Bruyn, A. G. *Nature* **264**, 222–226 (1976).
 13. Shostak, G. S. & van der Kruit, P. C. *Astr. Astrophys.* **132**, 20–32 (1984).
 14. Fujimoto, M. in *Interstellar Magnetic Fields* (eds Beck, R. & Gräve, R.) 23–29 (Springer, New York, 1987).
 15. Sofue, Y. in *Interstellar Magnetic Fields* (eds Beck, R. & Gräve, R.) 30–37 (Springer, New York, 1987).
 16. Ruzmaikin, A., Sokoloff, D. & Shukurov, A. *Nature* **336**, 341–347 (1988).
 17. Mathewson, D. S., van der Kruit, P. C. & Brouw, W. *Astr. Astrophys.* **17**, 468–486 (1972).
 18. Tilanus, R. P. J., Allen, R. J., van der Hulst, J. M., Crane, P. C. & Kennicutt, R. C. *Astrophys. J.* **330**, 667–671 (1988).

ACKNOWLEDGEMENTS. We thank R. Humphreys for an optical photograph of M83. The VLA is a facility of the National Radio Astronomy Observatory, which is operated by Associated Universities, Inc. under agreement with the NSF. The image reconstructions were carried out using the facilities of the National Centre for Supercomputing Applications at the University of Illinois; we thank R. Saul, M. Norman and R. Nandakumar for their help with the data processing and display of the images. S.S. was supported by the College of Liberal Arts and Sciences of the University of Illinois. We acknowledge the support of the NSF.

Detection of H₃⁺ on Jupiter

P. Drossart*, J.-P. Maillard†, J. Caldwell‡, S. J. Kim §, J. K. G. Watson||, W. A. Majewski||, J. Tennyson¶, S. Miller¶, S. K. Atreya*, J. T. Clarke#, J. H. Waite Jr** & R. Wagoner††

* Laboratoire Spatial (CNRS-URA264), Observatoire de Paris-Meudon, 92190 Meudon, France

† Institut d'Astrophysique, 98 Boulevard Arago, 75014 Paris, France

‡ Physics Department, York University, 4700 Keele Street, North York, Ontario M3J 1P3, Canada

§ Astronomy Program, University of Maryland, College Park, Maryland 20741, USA

|| Herzberg Institute of Astrophysics, National Research Council, Ottawa, Ontario K1A 0R6, Canada

¶ Department of Physics and Astronomy, University College London, Gower Street, London WC1E 6BT, UK

Department of Atmospheric, Oceanic and Space Sciences, Space Research Building, University of Michigan, Ann Arbor, Michigan 48109-2143, USA

** Department of Space Science, Southwest Research Institute, San Antonio, Texas 78284, USA

†† Department of Earth and Space Science, State University of New York, Stony Brook, New York 11794-2100, USA

SINCE their detection in the high latitudes of Jupiter, first by the Voyager Ultraviolet Spectrometer (UVS) experiment^{1,2}, then by the International Ultraviolet Explorer (IUE) satellite³, the auroral particle precipitations have been associated with various phenomena in the jovian environment. In the magnetosphere, the H₃⁺ ion, probably of ionospheric origin, was detected *in situ* by the Voyagers⁴. Infrared emissions were observed in spectral bands characteristic of CH₄ (ref. 5) and of other hydrocarbons^{6,7}, localized in two auroral spots^{5,8}. Here we present high-resolution spectra at a wavelength of 2 μm, in the southern auroral region of Jupiter, recorded at the Canada–France–Hawaii Telescope (CFHT), which we believe to be the first astronomical spectroscopic detection of H₃⁺. The derived rotational temperature of H₃⁺ is in the range 1,000–1,200 K. Such strong H₃⁺ lines could be used in future ground-based monitoring of the jovian auroral activity and to search for this molecular ion in the interstellar medium.

Observations of Jupiter were made at the CFHT with the Fourier Transform Spectrometer (FTS) during the night of 1988 September 24 (UT), between 2.0 and 2.2 μm, with a 5-arcsec aperture, at constant jovian latitude (60° S). We observed H₂ quadrupole ro-vibrational emission lines (S.J.K. *et al.*, manuscript in preparation) and determined the vibrational population of H₂ and the neutral temperature, 730 (+500/–200) K in the 0.1-μbar region. Figure 1 shows a calibrated interval of the

observed spectra in the 2-μm-wavelength window (the emission peak) which also comprise many strong emission lines. These lines are not present in the non-auroral spectrum, which is displayed for comparison. (Independent observations of some of these lines have been reported⁹ at low spectral resolution, both in north and south auroral regions.)

The strongest line, at 4,777 cm⁻¹, was monitored in individual spectra of 13-min integration each, for a total of 5 h. The emission comes from a region centred at a longitude of 60° (System III) and a latitude of 60° S. The variation of brightness with longitude (in System III), as the emitting region rotates through our stationary aperture, is reported in Table 1, along with the IUE data recorded almost simultaneously.

The IUE far-ultraviolet spectra were all taken at low dispersion with the large aperture, and the resulting H₂ spectra have been reduced and corrected for scattered light and jovian reflected sunlight using standard procedures^{3,10}. The auroral-emission brightness as a function of longitude indicates a moderately bright far-ultraviolet (FUV) aurora of 50–100 kRa (with the calibration of Table 1). The longitudinal dependence of the FUV and infrared emission brightnesses in the overlapping time period suggest a correlated process for the FUV and infrared emission. The complete reduction of the IUE observations, covering several days of September 1988, and the correlation with the mapping of the planetary disk at 7.8 μm will be published elsewhere (J.C. *et al.*, manuscript in preparation).

The rather irregular set of emission lines observed from Jupiter is reminiscent of the spectrum of a laboratory discharge through H₂ gas, in which the majority of lines belong to transitions between excited electronic states of the H₂ molecule^{11–13}. Comparisons with such spectra using various discharge sources showed, however, a significant number of coincidences for only one source, the cell used in ref. 14. This cell can operate at gas pressures up to ~50 torr and currents up to ~2.5 A. The pressure dependence of the intensities is used as a means of discriminating between the emission lines of the different species present in the plasma. Spectra taken at 10 and 50 torr showed that the relative intensities of the lines coincident with Jupiter lines generally increased with pressure, behaving in a similar way to the ro-vibrational lines of H₃⁺ (ref. 14) or the ro-electronic lines of neutral H₃ (ref. 15).

The 2-μm spectrum of this discharge cell was originally recorded in 1985 in a search for the 2ν₂ band of H₃⁺, which is predicted to be stronger in emission per molecule than the ν₂

TABLE 1 Comparison of infrared emission in H₃⁺ (4,777 cm⁻¹ line) and IUE H₂ (Lyman and Werner bands) from the southern hemisphere of Jupiter during the night of 1988 September 24

Jupiter longitude* (deg)	CFHT/FTS infrared intensity† (kRa)	IUE‡ image number	IUE ultraviolet intensity§ (kRa)
210–260	—	34,301	27
245–295	—	34,302	30
280–330	8.1	34,303	35
315–5	11.8	34,304	82
350–40	15.6	34,305	102
25–75	21.1	—	—
60–110	22.8	—	—

The IUE emission (recorded 1 h 15 min after the FTS data), has been scaled to the same aperture as the FTS observations, assuming an extended emission within a 5-arcsec disk. The intensities of the jovian lines were estimated from the calibrated spectrum (Fig. 1). The 1σ level is 4 kRa for the FTS observations (1 Rayleigh = 10⁶ photons cm⁻² s⁻¹).

* System III

† 4πl, 4,777 cm⁻¹ H⁺ line.

‡ Short Wavelength Primary camera.

§ 4πl, 1,230–1,620 Å, H₂ band.

TABLE 2 New emission lines in the spectrum of Jupiter

	Wavenumber Jupiter spectrum (cm ⁻¹)	Intensity (Jupiter) (W cm ⁻² sr ⁻¹) (×10 ⁻¹¹)	Wavenumber laboratory spectrum (cm ⁻¹)	Molecule	Wavenumber <i>ab initio</i> calculation (cm ⁻¹)	<i>J'</i>	<i>G'</i>	Assignment			Einstein coefficient <i>A_{ij}</i> (s ⁻¹)	
								<i>U'</i>	<i>J''</i>	<i>K''</i>		
1	4,497.841	1.81	4,497.8391	H ₂				q-S ₁ (0)				
2	4,554.238	3.56										
3	4,557.057	1.89		H ₃ ⁺	4,556.883	4	6	+2	4	3	o	35
4	4,586.282	2.64										
5	4,605.653	1.83										
6	4,638.361	5.26	4,638.338	H ₃ ⁺	4,638.688	10	12	+2	9	9	o	171
7	4,649.213	3.50										
8	4,664.274	3.29	4,664.303	H ₃ ⁺	4,663.949	2	3	+2	3	0	o	65
9	4,677.268	2.18	4,677.285	H ₃ ⁺	4,677.032	3	5	+2	3	2	p	43
10	4,685.582	4.30	4,685.558	H ₃ ⁺	4,685.694	9	11	+2	8	8	p	164
11	4,712.334	—	4,712.309	H ₃ ⁺	4,711.921	5	5	+2	5	2	p	68
12	4,712.882	5.31	4,712.9054	H ₂				q-S ₁ (1)				
13	4,732.050	4.63	4,732.053	H ₃ ⁺	4,732.158	8	10	+2	7	7	p	158
14	4,777.215	12.20	4,777.228	H ₃ ⁺	4,777.123	7	9	+2	6	6	o	151
15	4,795.018	2.10		H ₃ ⁺	4,794.697	2	4	+2	2	1	p	56
16	4,804.463	3.46	4,804.406	H ₃ ⁺	4,804.080	3	4	+2	3	1	p	70
17	4,816.415	3.02	4,816.361	H ₃ ⁺	4,815.465	4	0	-2	5	3	o	89
18	4,820.542	3.90	4,820.616	H ₃ ⁺	4,820.503	6	8	+2	5	5	p	144
19	4,861.839	—	4,861.849	H ₃ ⁺	4,861.606	5	7	+2	4	4	p	136
20	4,862.385	—										
21	4,876.912	5.60	4,876.99 sh	H ₃ ⁺	4,876.231	2	1	-2	3	2	p	98
22	4,895.498	6.56	4,895.520	H ₃ ⁺	4,895.237	8	9	+2	7	6	o	123
23	4,898.534	6.52										
24	4,899.046	3.42										
25	4,900.377	12.85	4,900.393	H ₃ ⁺	4,900.138	4	6	+2	3	3	o	127
26	4,907.000	3.42										
27	4,907.859	7.90	4,907.869	H ₃ ⁺	4,907.381	1	3	+2	1	0	o	155
				H ₃ ⁺	4,907.827	3	0	-2	4	3	o	100
				H ₃ ⁺	4,913.634	3	3	+2	3	0	o	148
28	4,914.247	7.74	4,914.21 sh	H ₃ ⁺				q-S ₁ (2)				
29	4,916.904	2.08	4,917.0069	H ₂								
30	4,931.561	9.12	4,931.604	H ₃ ⁺	4,931.277	7	8	+2	6	5	p	118
31	4,935.946	8.12	4,935.969	H ₃ ⁺	4,935.667	3	5	+2	2	2	p	114
32	4,966.859	—	4,966.862	H ₃ ⁺	4,966.504	6	7	+2	5	4	p	111
33	4,971.537	—	4,971.559	H ₃ ⁺	4,970.645	2	0	-2	3	3	o	141
34	4,975.396	—										
35	4,997.561	—										
36	5,000.527	—	5,000.506	H ₃ ⁺	5,000.138	5	6	+2	4	3	o	101

List of the 36 new emission lines brighter than a 3σ threshold above the continuum, detected in the original spectrum of Jupiter before calibration, compared with the laboratory spectral lines and *ab initio* calculations. Missing intensities in Jupiter lines correspond to lines detected in the uncalibrated spectrum, but with large uncertainties in the calibration procedure (for weak lines or telluric line contamination). In the intensity fit two lines (4,820 and 4,931 cm⁻¹) are removed, because of probable interference by telluric and other jovian lines.

sh=shoulder on an H₂ line; o=ortho (nuclear spin weight 4); p=para (nuclear spin weight 2).

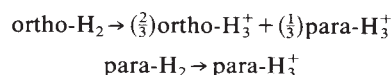
fundamental¹⁶. The high rotational temperature, however, together with the possibility that the lines might be due to neutral H₃, prevented definite assignments until improved *ab initio* predictions¹⁷ and an observation of the 2ν₂-ν₂ difference band¹⁸ became available. A model Hamiltonian¹⁹ fitted to these data allowed initial assignments. The *ab initio* calculations have now been extended to higher values of *J* (S.M. and J.T., manuscript in preparation), making it possible to assign a total of about 50 of the laboratory lines (A.M. *et al.*, manuscript in preparation) and 23 of the Jupiter lines, most of which coincide with a laboratory line. The Jupiter emission lines in this wavelength region therefore belong predominantly to the 2ν₂ band of H₃⁺ (Table 2).

The laboratory wavenumbers for the H₃⁺ lines were calibrated against lines of H₂ and have an uncertainty of the order of 0.01 cm⁻¹. A small residual line shift on the Jupiter lines can be accounted for by a slight offset (2 arcsec) of the aperture relative to the central meridian. The *ab initio* wavenumbers are on average 0.297 (±0.061) cm⁻¹ lower than the Jupiter wavenumbers, with a standard deviation of 0.297 cm⁻¹ about this mean.

Because the optical depth of the H₃⁺ lines is expected to be low (see below), the intensities of the lines are just proportional to the number of atoms in the upper states. The intensities were fitted following standard procedures of infrared spectroscopy²⁰,

allowing for a fraction *f_p* of para levels and *f_o* = 1 - *f_p* of ortho levels. (The equilibrium values at high temperatures are *f_p* = *f_o* = 0.5.) Using the *ab initio* Einstein coefficients *A_{ij}*, the observed Jupiter intensities gave the rotational temperature, the para fraction *f_p* and the column density (that is, the concentration integrated along the path length). The best fit to the data of Table 2 gives: column density = 1.39 (±0.13) × 10⁹ cm⁻²; *T_r* = 1099 (±100) K; *f_p* = 0.58 (±0.03). The column density here refers to H₃⁺ ions in the 2ν₂(*l* = 2) vibrational state.

In the formation reaction for H₃⁺ (reaction (1) below), it is usually assumed that the weaker H₂⁺ bond is broken and that the ratios of the nuclear-spin modifications of the H₃⁺ produced therefore reflect those in the initial H₂ molecules according to the following relations²¹:



From the observed *f_p* of H₃⁺ we derive:

$$f_p(\text{H}_2) = [3f_p(\text{H}_3^+) - 1]/2 = 0.37(\pm 0.05)$$

This would be the equilibrium ratio at a temperature of ~106(±20) K, and is only a little higher than the measured

$f_p(\text{H}_2)$ in the troposphere²².

The primary mechanism for the production of H_3^+ in the atmosphere of Jupiter is the following reaction²³



(with $k = 2.0 \times 10^{-9} \text{ cm}^3 \text{ s}^{-1}$, ref. 24). In the auroral region H_2^+ is produced principally by electron impact with H_2 (ionization by solar EUV is negligible):



The loss of H_3^+ occurs by the following dissociative recombination reactions:



or



The rate of reaction (3) is controversial at present, but the latest measurement is $1.8 (\pm 0.2) \times 10^{-7} \text{ cm}^3 \text{ s}^{-1}$ (ref. 25) which is in agreement with ref. 26 but not with ref. 27 ($\leq 10^{-11} \text{ cm}^3 \text{ s}^{-1}$). Using the larger rate constant the H_3^+ column abundance is calculated to be $6 \times 10^{10} \text{ cm}^{-2}$ in a non-auroral EUV-controlled ionosphere^{28,29}. In the jovian auroral region, however, $\sim 10^{13} \text{ W}$ of power is deposited²⁹, which corresponds to an energy flux of $10^{-6} \text{ W cm}^{-2}$. Ionization caused by the 1–10 keV electrons at this energy flux is expected to result in an H_3^+ column abundance as high as $6\text{--}10 \times 10^{12} \text{ cm}^{-2}$, with a factor of 2–3 uncertainty

resulting from uncertainties in the energy deposition rates, the chemical rate constants and the peak electron concentration. The Maxwellian tail of the auroral electron energy distribution can provide the required ion-production rates above the ionospheric maximum. Assuming H_3^+ is the major ion, its column abundance is found to be $\geq 5 \times 10^{12} \text{ cm}^{-2}$ from the Voyager ionospheric measurements in the auroral region (67°S)³⁰. Using these estimates of the H_3^+ column density and the Einstein coefficients of Table 2, the optical depth in a strong H_3^+ line is found to be $< 10^{-3}$, as assumed in the intensity fit. The IUE emission reported in Table 1 is consistent with the model of ref. 29, from which the column abundance of H_3^+ is calculated.

There are two possible classes of mechanisms for populating the upper state of the transition. First, non-thermal processes: direct excitation mechanisms may be invoked, such as a transition between $\text{H}_2(v=1)$ (with a non-thermal population), and H_3^+ ; second, thermal processes—the population of the upper level could simply be the thermal population, in a high-temperature atmospheric level, with $T \approx 1,100 \text{ K}$. Thermal collisions are efficient only for large values of the parameter ϕ , the ratio of the inelastic-collision time to the radiative lifetime, derived from the Einstein coefficient. Using the rough estimates of $2.7 \times 10^{-10} \text{ cm}^3 \text{ s}^{-1}$ for the rate of vibrational quenching of H_3^+ by H_2 (ref. 31) and for atmospheric pressure between 1–100 nbars (ref. 29), ϕ is found in the range 0.1–4. Therefore, if the neutral temperature is as high as 1,100 K (ref. 29), a thermal population of the upper level of the $2\nu_2$ band of H_3^+ could account for the calculated column density of H_3^+ in the upper vibrational state. To discriminate between these possibilities further observations, such as the Doppler resolution of the H_3^+ lines (a measure of the translational temperature) or the observation of other vibrational bands of this ion, are required. □

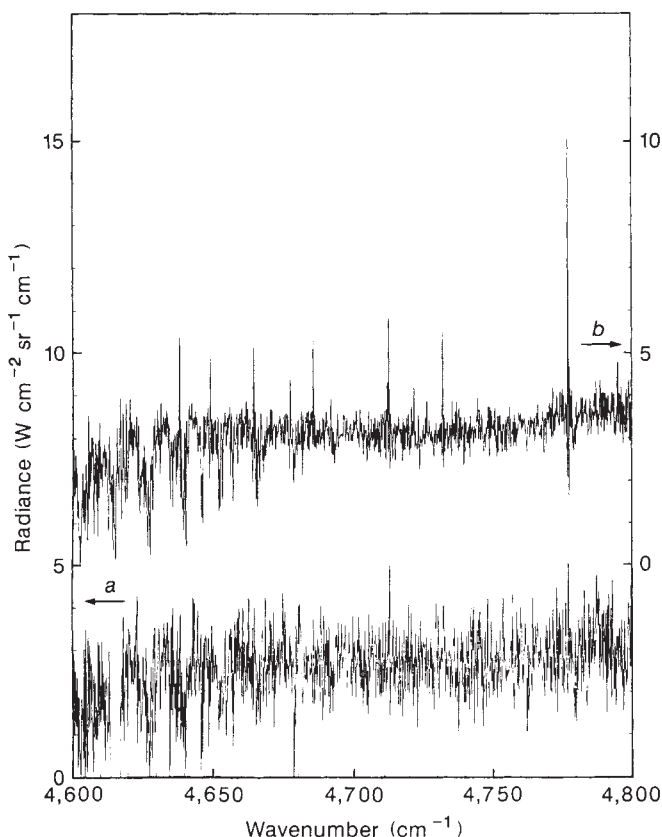


FIG. 1 FTS Spectra of Jupiter (24 September 1988, ut) recorded at constant latitude (60°S), with a 5-arcsec aperture kept centred on the central meridian of the jovian disk. *a*, For a non-auroral spot (longitude: 284° ; integration time: 13 min; signal to noise = 7) and *b*, for an average of the auroral spectra (mean longitude 60° ; total integration time: 90 min; signal to noise = 18). Spectral resolution is 0.23 cm^{-1} (FWHM). Calibration is performed by comparison with a standard star (θ_2 Tau, Bright Star 1412, K magnitude = 2.92).

Received 2 May; accepted 10 July 1989.

- Broadfoot, A. L. *et al. Science* **204**, 979–982 (1979).
- Sandel, B. R. *et al. Science* **206**, 962–966 (1979).
- Clarke, J. T., Moos, H. W., Atreya, S. K. & Lane, A. L. *Astrophys. J.* **241**, L179–L182 (1980).
- Hamilton, D. C. *et al. Geophys. Res. Lett.* **7**, 813–816 (1980).
- Caldwell, J., Tokunaga, A. T. & Gillett, F. C. *Icarus* **41**, 667–675 (1980).
- Kim, S. J., Caldwell, J., Rivolo, A. R. & Wagener, R. *Icarus* **64**, 233–248 (1985).
- Drossart, P. *et al. Icarus* **66**, 610–618 (1986).
- Caldwell, J., Hallthore, R., Orton, G. S. & Bergstrahl, J. *Icarus* **74**, 331–339 (1988).
- Trafton, L., Lester, D. F. & Thompson, K. L. *Astrophys. J.* (in the press).
- Skinner, T. E. & Moos, H. W. *Geophys. Res. Lett.* **11**, 1107–1110 (1984).
- Crosswhite, H. M. *The Hydrogen Molecule Wavelength Tables of Gerhard Heinrich Dieke* (Wiley-Interscience, New York, 1972).
- Herzberg, G. & Jungen, Ch. *J. chem. Phys.* **77**, 5876–5884 (1982).
- Senn, P., Quadrelli, P., Dressler, K. & Herzberg, G. *J. chem. Phys.* **83**, 962–968 (1985).
- Majewski, W. A., Marshall, M. D., McKellar, A. R. W., Johns, J. W. C. & Watson, J. K. G. *J. molec. Spectrosc.* **122**, 341–355 (1987).
- Majewski, W. A. & Watson, J. K. G. in *42nd Symposium on Molecular Spectroscopy* (ed. Rao, K. N.) WF4 (Ohio State University, Columbus, 1987).
- Carney, G. D. & Porter, R. N. *J. chem. Phys.* **65**, 3547–3565 (1976).
- Miller, S. & Tennyson, J. *J. molec. Spectrosc.* **128**, 530–539 (1988).
- Bawendi, M. G., Rehfuss, B. D. & Oka, T. *43rd Symposium on Molecular Spectroscopy* (ed. Rao, K. N.) RA10 (Ohio State University, Columbus, 1988).
- Watson, J. K. G. *J. molec. Spectrosc.* **103**, 350–363 (1984).
- Herzberg, G. *Infrared and Raman Spectra of Polyatomic Molecules* 509 (Van Nostrand, Princeton, 1945).
- Quack, M. *Mol. Phys.* **34**, 477–504 (1977).
- Conrath, B. J. & Gierasch, P. J. *Icarus* **57**, 184–204 (1984).
- Atreya, S. K. *Atmospheres and Ionospheres of the Outer Planets and Their Satellites*, 121–142 (Springer, Berlin, 1986).
- Theard, L. P. & Huntress, W. T. *J. chem. Phys.* **60**, 2840–2848 (1974).
- Amano, T. *Astrophys. J.* **329**, L121–L124 (1988).
- Leu, M. T., Bondi, M. A. & Johnsen, R. *Phys. Rev.* **A8**, 413–419 (1973).
- Adams, N. G. & Smith, D. *IAU Symp. No. 120: Astrochemistry* (eds Vardya, M. S. & Tarufdar, S. P.) 1–18 (Reidel, Dordrecht, 1987).
- Atreya, S. K. & Donahue, T. M. in *Jupiter* (ed. Gehrels, T.) 304–318 (University of Arizona Press, 1976).
- Waite, J. H. Jr *et al. J. geophys. Res.* **88**, 6143–6163 (1983).
- Eshleman, V. R. *et al. Science* **206**, 959–962 (1979).
- McConnell, J. C. & Majeed, T. *J. geophys. Res.* **92**, 8570–8578 (1987).

ACKNOWLEDGEMENTS. We thank M. G. Bawendi, B. D. Rehfuss and T. Oka for information prior to publication, P. A. Feldman, G. Herzberg, and I. Dabrowski for discussions and comparisons between hydrogen discharges under various conditions and M. Vervloet for measurements and new spectra taken to test whether some of the Jupiter lines might be due to neutral H_3 . We also thank G. Tarrago for preliminary calculations on this band of H_3^+ , and C. Griffith for contributing to IUE data acquisition.